Investigation of Slotted Ground and M-Shaped DGS in Enhancing MIMO Antenna Isolation

K. V. Prasad[1] · Venkata Siva Prasad Makkapati[2]

Abstract

MIMO antennas, due to their compact size, are widely used for wireless applications. The isolation or mutual coupling (MC) between MIMO elements is still a research problem. The spacing between the elements will be minimized to accomplish system compactness, which allows for high MC between the elements. This paper presents a new 2-element MIMO design with slotted patch elements using M-shaped DGS for the MC reduction. The feed used is strip-line feed, and the design is simulated using HFSSv15. With a slot cut in all the square patch's four directions, the MIMO design is simulated using HFSS. The ground plane design will alter the antenna parameters to the required level based on the parametric patch analysis. The structure comprises two elements on a 50×36 mm^2 FR4 substrate. The effects of slots on gain and bandwidth are demonstrated. An M-shape DGS and a slot cut in all directions reduce this new design's MC. The proposed structure resonates at 3.5 GHz (WiMAX), 5.9 GHz (WLAN), 7.9 GHz (X-band SATCOM applications), and 9.3 GHz (Radar, Mobile phones, and commercial WLAN) in the entire Ultra-Wide Band (UWB) range and therefore achieves multi-band characteristics. The spacing between elements is 11 mm. A 20 dB MC reduction is achieved at the operating multi bands. The proposed design structure achieves ECC < 0.04 and DG > 9.985.

Keywords Defected ground structure (DGS) · Diversity gain (DG) · Envelope correlation coefficient (ECC) · Mimo · Patch · Slits

1 Introduction

In [1], a compact monopole antenna is designed for UWB frequency. The proposed design with substrate dimensions $25 \times 18 \times 1.6$ mm^3 utilizes two kite-shaped elements in coalesced form with the tapered slotted ground. The parametric analysis of the kite-shaped patch and the tapered base is made, an Impedance Bandwidth (IBW) of 14.2 GHz is accomplished,

✉ K. V. Prasad
   prasadkv@vrsiddhartha.ac.in

   Venkata Siva Prasad Makkapati
   mvsprasad@rvrjc.ac.in

1   ECE, V R Siddhartha Engineering College, Vijayawada, Andhra Pradesh 520007, India

2   ECE, R V R & J C College of Engineering, Chowdavaram, Guntur, Andhra Pradesh 522019, India

and the gain is in the range of 2.28–5.0 dBi for the entire UWB. In [2], a hexagonal-shaped MIMO antenna is analyzed and studied, covering the S-band, WLAN, UWB, and X-band. The substrate used is FR4 with dimensions $0.18\lambda_0 \times 0.37\lambda_0$. The distance between the two patches is $0.053\lambda_0$. Triangular-shaped-edge-cuttings are made in the design bottom, and DGS is used. Isolation is enhanced by 20 dB with an E-shaped tree arrangement and parasitic elements. Various MIMO parameters like ECC, DG, and Total Active Reflection Co-efficient (TARC) are measured for the operating frequency bands. In [3], a compact Minkowski design for reducing MC in between two elements is analyzed. The proposed MIMO design, which resonates at 2.5, 3.5, 5.2, and 7 GHz frequencies, shows the reduction in MC with 54, 50, 40, and 44 dB at the resonating frequencies. In [4], the miniaturization of the antenna design with gain enhancement is proposed with Modified Minkowski Fractal DGS (M-MFDGS) for three patch antennas with different feeding techniques. The design with strip-line feeding provides 70% patch area reduction with a gain of 1.43 dBi.

The design with proximity-coupled feeding achieves a higher gain and bandwidth (5.11 dBi and 110 MHz). The design with aperture coupled feeding provides a gain of 5.91 dBi. In [5], a compact patch with M-MFDGS for 2.4 GHz WLAN application is proposed. Incorporating capacitive M-MFDGS, without changing the dimensions of the patch, the operating frequency is shifted from 4.16 GHz to 2.4 GHz. The design dimensions are 0.15 $\lambda_0 \times 0.13~\lambda_0$, with IBW of 5.20%, and gain of 1.4 dBi centered at 2.41 GHz. This design is suitable for portable wireless applications.

In [6], a four-port monopole design is analyzed for MIMO applications. To enhance bandwidth, the structure is studied by making an arrow-shaped slot etched on the radiator and stepped ground. In [7, 8], a band-notched miniaturized Printed Log Periodic Dipole Array (PLPDA) with a meander fractal concept is proposed for wide-band applications. This concept is applied to all the elements in the PLPDA. Using the sub-sectional tapered concept, band notch characteristics are obtained in the WLAN band, WiMAX band, and a broad bandwidth with this meander fractal concept. The proposed design, fabricated on a RO3003 substrate, is best applicable for short-range, high-speed wireless communications. In [9], a modified radiating patch with high-gain broadband using a Poly tetra fluoro ethylene (PTFE) substrate is proposed. Dimensions for the design are $0.52\lambda_0 \times 0.51\lambda_0$. Gain and BW effects are analyzed using a slot and five slits on the proposed antenna element design. In [10], resistor-loaded paired parallel-coupled resonators (PCRs) are used for isolation enhancement in MIMO elements. The spacing between array elements is $0.125\lambda_0$, and isolation greater than 25 dB is achieved within the UWB.

In [11], to achieve better data rates with enhanced gain for the 5G communications, the antenna design is made with a substrate, Polymethacrylate. This substrate provides a high gain compared to all the other substrates used in the antenna design. A gain of 10.054 dB with a bandwidth of 80 MHz is achieved with this substrate. The patch antenna with this substrate is preferred for 5G cellular base station (BS) antenna for the frequency range of 3.3 GHz–3.7 GHz. These high gain antennas are designed with two simple techniques: Simple shorting pin and chip impedance shorting. The overall geometry of the patch antenna is reduced with a simple shorting pin technique with improved gain, and the narrowband effect can be minimized by implementing the chip impedance shorting method. The design with high gain is best suitable for 5G cellular communications. In [12], a novel design structure, Spiro Meander Line Uniplanar Compact Electromagnetic Band Gap (SMLUC-EBG), is presented. This design is proposed to minimize MC between elements for WLAN applications. The spacing between the elements is $0.14\lambda_0$, and isolation of 20.3 dB is achieved with the proposed design. In [13], a circular patch antenna for WLAN application is presented with an eroded ground plane, and it is electromagnetically

coupled. The eroded ground plane minimizes the physical area of the circular patch and can be utilized for WLAN services. The miniaturized antenna provides excellent reflection characteristics at a 2.4 GHz frequency. In [14], a circular annular ring patch by embedding an Electromagnetic Band Gap (EBG) structure reduces surface waves. An M-shaped EBG is utilized on the ground with vias at the center of each EBG, and this EBG is inscribed in the 6×6 mm^2 patch. This proposed design can be utilized for the Mobile Satellite Service (MSS) band, UMTS, and WCDMA. In [15], a dual-band patch for WLAN and WiMAX applications are presented with narrow vertical slots. The proposed antenna with two vertical slots resonates at 3.5 GHz WiMAX and 5.3 GHz WLAN bands. Particle Swarm Optimization (PSO) method is incorporated to optimize the proposed design dimensions. This design provides better radiation properties at the two bands, making it appropriate for dual-band implementation. In [16], threefold stubs are etched to reduce MC between elements. This design consists of two polyhedron annulus patch elements, threefold fork-shaped stubs (TFSS), a conventional dielectric substrate, and a microstrip line feeder. By using this TFSS, the performance parameters are improved. MC was improved by 42 dB when the TFSS and polyhedron annulus patch elements were introduced. In [17, 18], three patch antennas are designed with direct, proximity, and aperture coupled feeding for X-band portable applications by loading the M-MFDGS technique. The overall physical size of the patch with these feeding techniques and M-MFDGS reduces up to 67% and overall volumetric reduction of 84%. The gain of this proposed design is about 6.2 dBi at 10 GHz. In [19], a compact design with the partial ground and parasitic elements and a rectangular slot on the I-shape element is proposed. The FR-4 substrate dimensions of the proposed technique are $15 \times 20 \times 1.6$ mm^3. This design provides bandwidth enhancement. Simulated results show that the IBW was achieved at three resonant frequencies. This antenna design is suitable for Wi-Fi, WiMAX, and X band. In [20], a novel periodic defected ground structure of S-shape (PDGS) to reduce MC between elements is proposed with three S-shaped DGS structures placed between the elements, and the spacing is 50 mm. With this arrangement, a 40 dB reduction in MC is achieved. PDGS interrupts the far-field and induces current between the elements, and etched PDGS minimizes the surface current considerably within a restricted substrate area.

In [21], compact EBG integrated MIMO is proposed for WLAN and WiMAX to reduce MC between the elements, and the proposed design operates within the range 2.01–3.92 GHz. The proposed MIMO design has very low ECC, good DG, very low Channel Capacity Loss (CCL). In [22], a DGS used to suppress MC in MIMO design is presented, and this design eliminates the phased array scan blindness. By analyzing, the surface waves will get squashed in the substrate using back-to-back U-shaped DGS. In [23], a compact UWB-MIMO with low MC is introduced and is designed with 50×30 mm^2. In this design, F-shaped stubs maintain isolation between the elements. This design has S21 < −20 dB, better ECC, DG, over the UWB frequency. In [24], in a slot array, a metamaterial is used for steering the surface waves so as to reduce MC. Both Complementary Split Ring Resonator (CSRR) and complimentary fishnet structures are used to minimize MC. An isolation improvement of 14 dB is obtained throughout 2 GHz bandwidth, with a 3.4 mm slot gap. In [25], a novel fractal DGS to minimize MC between coplanar elements is proposed, and the bandgap characteristic of the design is studied. Results show that isolation enhancement of > 35 dB is obtained. In [26], a compact design for UWB is investigated. This design implementation is performed with a patch and parasitic elements at the top, and DGS is etched on the substrate bottom. The proposed design dimensions are $20 \times 20 \times 1.6$ mm^3 with an efficiency of 79.8%, respectively. It is best suitable for WiMAX, WLAN. In [27], a MIMO antenna design for reducing MC is proposed. Six

parallel metal strips are introduced between two patches to reduce MC between the elements, and -42 dB is achieved with metal strips at 5.8 GHz frequency. In [28], an effective technique of utilizing metallic pins at the square element edges to alter the antenna polarization is proposed. The measurements indicate that the isolation enhances from 2.8 dB to 20 dB at 3.5 GHz. In [29], to reduce the MC, an EBG is used as an isolator and is of about 30.5 dB and provides low ECC. In [30], a compact design with improved isolation consists of slot antennas with 22×26 mm^2. A T-shape slot is etched on the ground to provide better impedance matching and reduce the MC. The design provides MC of < -18 dB over the UWB. In [6], dual-band MIMO elements that operate at 3.7 and 4.1 GHz is presented. The MIMO element spacing is about 0.034λ0. The design consists of a decoupling surface and H-shaped DGS. The isolation is greater than 30 dB in both 3.7 and 4.1 GHz bands from the decoupling structure and the DGS.

In [31], a UWB-MIMO design that provides good dual-band suppression with port isolation is presented. This design utilizes a fractal-shaped patch, parasitic neutralization stubs, ground, and notches to achieve band notches at WiMAX and X-band. In [32], a four-port monopole is presented using arrow-shaped slot etching and step etching to enhance isolation and bandwidth. The ECC obtained was less than 0.001 and the efficiency was greater than 85.70%. In [33], a slit embedded mushroom EBG and periodical CSRRs are implemented to reduce surface waves between elements. An H-shape DGS is introduced to reinforce the decoupling effect, and a12 dB MC reduction is realized. In [34], a two-element miniaturized MIMO antenna with reduced MC is presented. MIMO antenna is simulated with four T-shaped slots on the patch with 50×25 mm^2 on FR-4 epoxy. A T-shape ground stub and a slot reduce the MC of the proposed method. This provides multi-band characteristics for the applications like WiMAX, WLAN, X-band SATCOM and Radar, Mobile phones, and WLAN.In [35], applications like WLAN, Wi-MAX are studied. In [36], a miniaturized slot-shaped EBG design structure with cell dimensions, 6.3×6.3 mm^2 is proposed. This proposed design analyses the surface wave effects in the antenna array resonating at 5.8 GHz frequency. The slot-shaped design will modify the S-parameters with $S_{11} < -10$ dB and $S_{12} < -51$ dB and changes the surface current distribution to avoid surface waves. This miniaturized structure is best suitable for the WLAN application.

The remainder of the paper is organised as follows: The antenna analysis with different parameters is described in Sect. 2. Section 3 deals with the results of the design proposed. The conclusion is presented in Sect. 4

2 Antenna Design and Analysis

Figure 1 represents a MIMO design with slits on all four sides of the patch. The proposed structure simulation is performed on FR-4 substrate with Ws×Ls (36×50 mm^2), tan δ=0.002, εr=4.4. The height of the substrate is 1.6 mm. An M-shaped DGS between two radiators for isolation enhancement is shown in Fig. 1. This design uses Lp×Wp (Lp=Wp) patch element, four slits on all the sides with L length and N width. The proposed structure is excited with strip-line feed, and inter-element spacing is approximately 11 mm, between the two MIMO elements.

The upper patch and the ground structure of the proposed design is shown in Fig. 2.

As it is a square patch, length and width are identical. Figure 1 depicts a MIMO antenna fed with strip-line, uses four cross-shaped slots on four sides of the antenna element, with
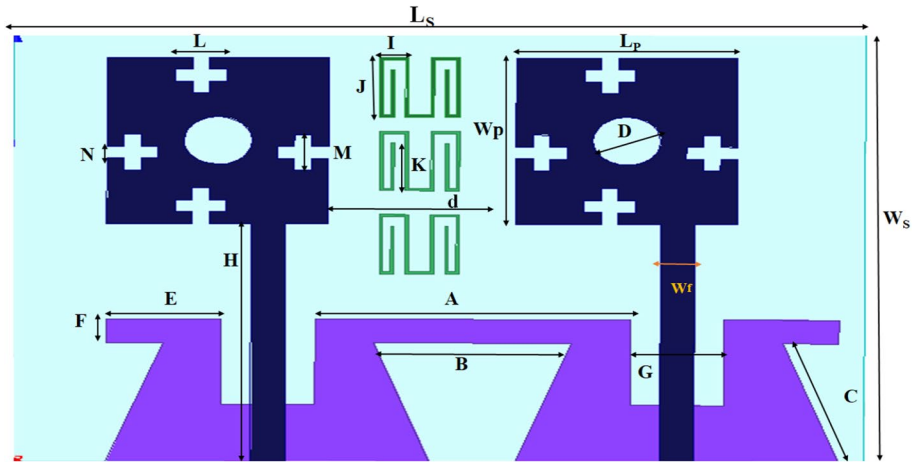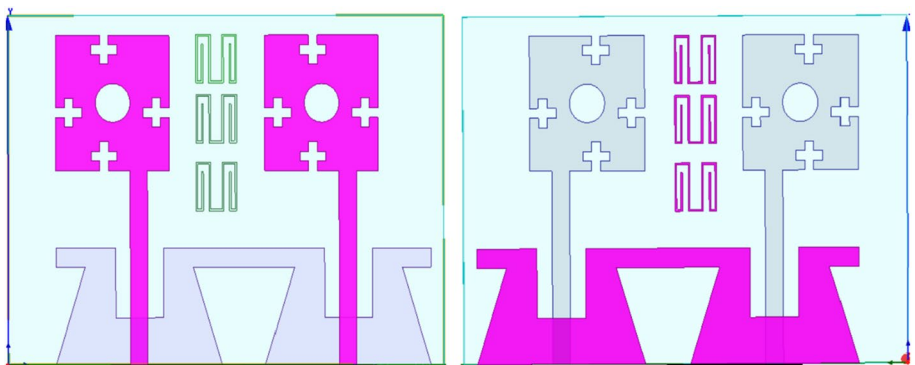
Fig. 1 A Proposed MIMO structure

Fig. 2 Upper patch and ground plane of the proposed design

two different sizes, length L and width N. The upper patch and ground plane is represented in Fig. 2.

The antenna design is simulated using HFSS 15.0 and fabricated on FR-4 substrate with a thickness (height) of 1.6 mm, length and width, Ws × Ls. An M-shaped DGS between two cross-shaped elements is indicated in Fig. 1. The design implements a patch with different sizes of cross-shaped slots are etched on the four directions of the patch with length L (where L = M) and width N. The edge-to-edge distance between the elements is 11 mm. Multiple slits are introduced for the MIMO element, and the design operates for the UWB with specific applications at WiMAX, WLAN, X-band SATCOM, and commercial WLAN. The simulated S_{11} and S_{12} plots for the proposed technique are shown in Fig. 3. The optimized parameters are listed in Table 1. As the notations provided in the Table 1, Ls and Ws indicates the substrate length and width. Lp and Wp denotes the patch length and width. A, B, C, E, F, and G denotes the slotted ground dimensions. D indicates the diameter of the circle. L, M, and N provides the slit length and width. I, J, and K denotes the M-shaped DGS length and width. d denotes the
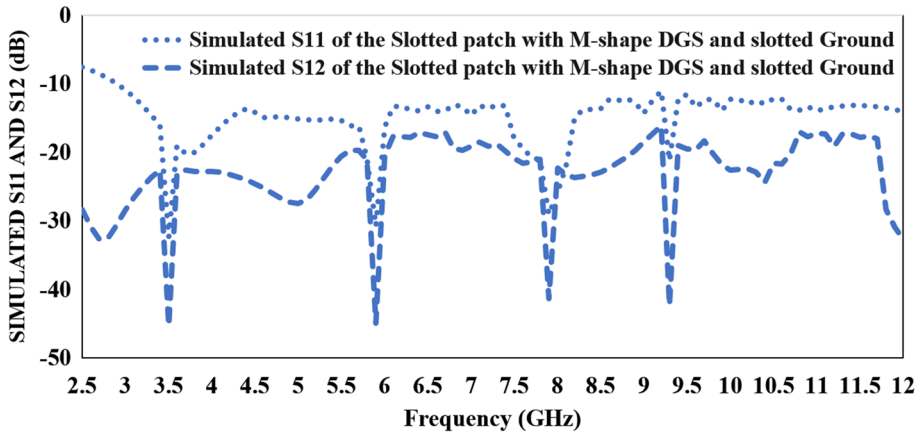
Fig. 3 Proposed S_{11} and S_{12} of the design

Table 1 Proposed design Parameters

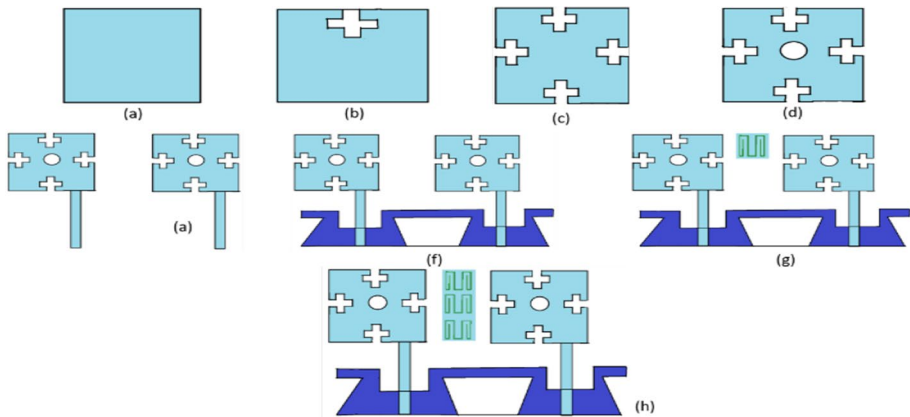| Parameter	L_S	Ws	Lp	Wp	A	B	C	D	G
Value (mm)	50	36	15	15	18	11.5	10	4	5.5
Parameter	H	I	J	K	L	M	N	Wf	
Value (mm)	20	1.7	5	4	3	3	1	2	

Fig. 4 Formation steps of the design

edge-to-edge spacing between the patch elements and W_f denotes the width of the feed line. H denotes the feedline height.

Finally, the proposed design with $|S_{11}| < -10$ dB, resonating from 2.5 GHz to 12 GHz, is plotted in Fig. 4(h). Isolation of < -20 dB is observed. The simulation is performed for all the evolution design steps of the proposed design, and S_{11} for the iterations is shown in Fig. 5
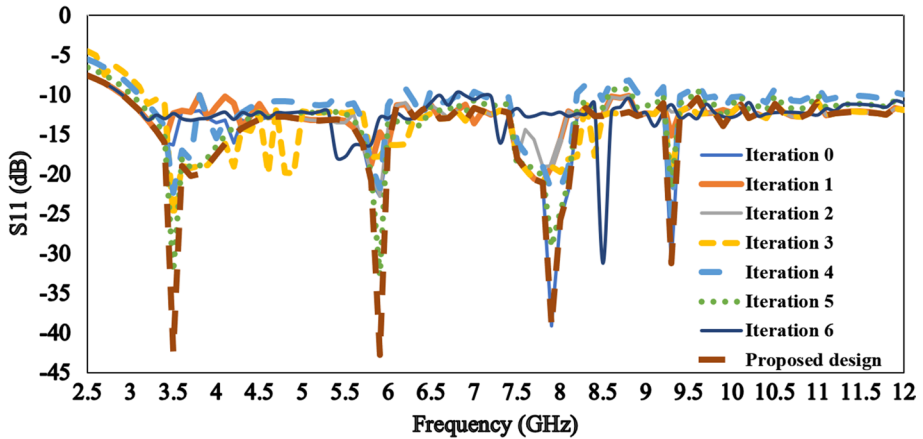
Fig. 5 S_{11} Iterations

From iteration 0 to the proposed method, S_{11} is plotted and is represented in Fig. 5. For iteration 0 S_{11} is approximately at -12 dB. As the iterations are increased from iteration 0 to the proposed design the return loss achieves better performance and the peaks occurs at four different resonant frequencies.

2.1 Effect of Slits on Patch Element

The concept of DGS used in MIMO is proposed in ref. [11, 13, 14, 17] and in [21]. Defected Ground Structure (DGS) acts as a band stop filter that blocks the surface currents flowing in the desired frequency from one radiator to another. From the design analysis, the proposed DGS provides good MC reduction. The S-parameters with and without Slotted ground and M-shaped DGS are compared in Figs. 6,7. From Fig. 6, using an M-shaped DGS and the slits on the patch, the peaks at which the antenna
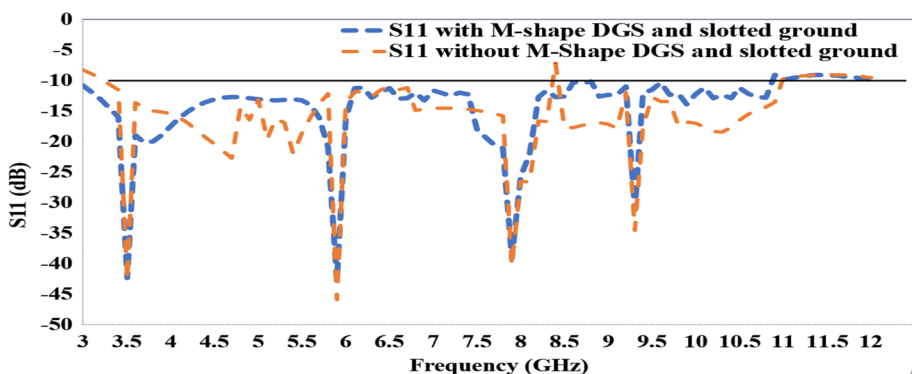

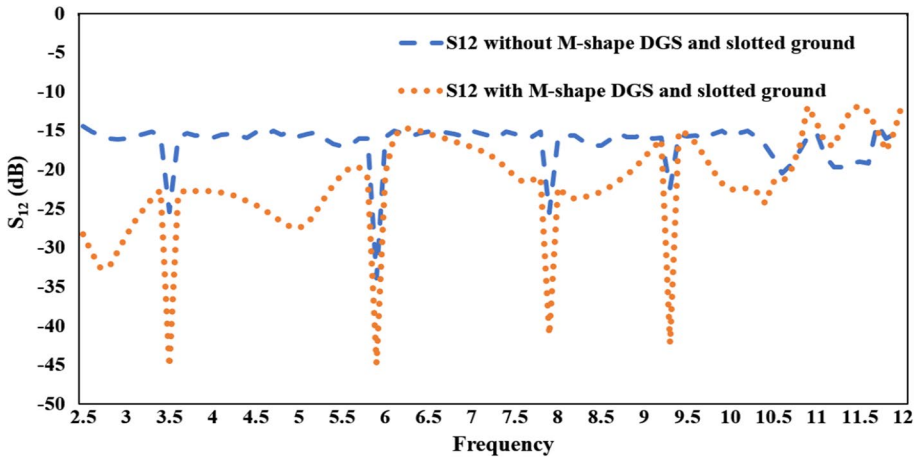**Fig. 6** Simulated S_{11} with and without M-shaped DGS and slotted ground

Fig. 7 S_{12} of the proposed design with and without slotted ground and M-shape DGS

resonates are 3.51 GHz, 7.95 GHz, and 9.45 GHz. $S_{12} > -15$ dB is achieved over the UWB range.

2.2 Slotted Ground and DGS Effects on the Proposed Design

Figures 6, 7 shows S_{11} and S_{12} parameters with and without M-shape DGS and slotted ground.

A slotted ground is used to enhance isolation. From the S_{11} plot, the peaks at which the antenna resonates are 3.51 GHz, 7.95 GHz, and 9.45 GHz using a slotted ground. Etching slots on the ground edges enhance S_{12} with the slotted ground structure. MC is reduced at the resonating peaks that make $S_{12} > -15$ dB.

2.3 Parametric Analysis of the Design Proposed

Isolation improvement of the design is analyzed based on the parametric analysis by performing the slit length variation on the patch element and varying the distance between the patch radiators. The scattering parameters $|S_{11}|$ & $|S_{12}|$ for different distances are analyzed in Fig. 8. In this design, parametric analysis has been done by varying one parameter, and all other parameters remain unchanged to evaluate S-parameters.

2.3.1 Effect On Distance Variation

The distance variation affects S_{11} with d = 7.5 mm to d = 11 mm, and the S_{11} variation to the distance between the patches is shown in Figs. 8, 9. From Fig. 8, distance, d = 11 mm, will resonate the antenna at 3.5 GHz, 5.9 GHz, 7.9 GHz and 9.3 GHz and S_{11} at these resonating frequencies are -42.62 dB, -45.84 dB, -40.23 dB and -34.56 dB
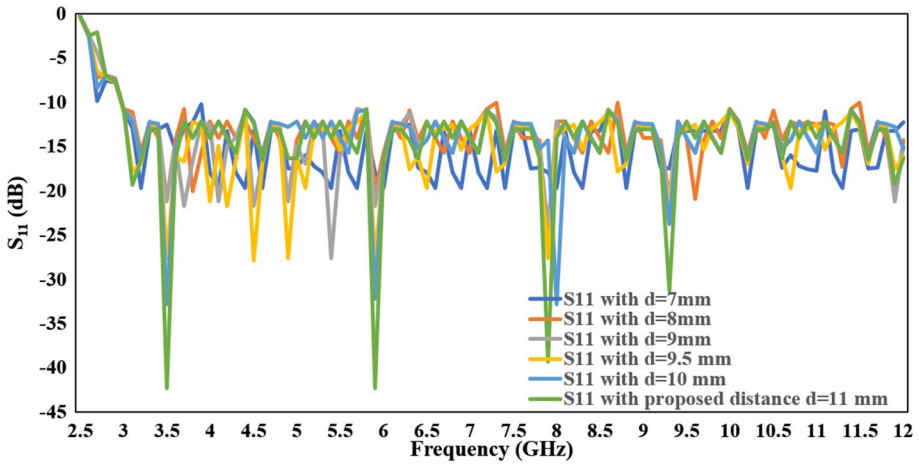
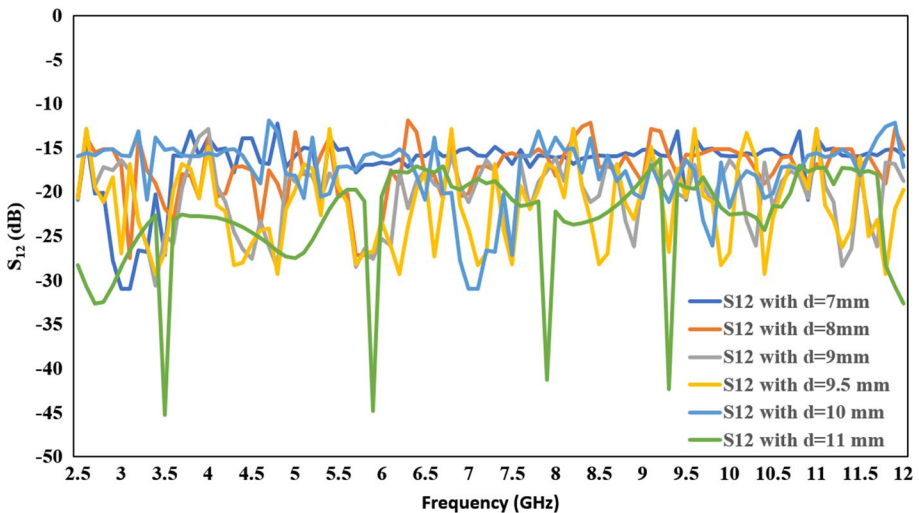**Fig. 8** S_{11} for distance variation of the MIMO design

Fig. 9 S_{12} with different distances for the proposed antenna

and S_{12} at these frequencies are − 45.26 dB, − 44.83 dB, − 41.25 dB and – 42.31 dB and are depicted in Fig. 9. The spacing between the elements, d = 11 mm, S_{11} & S_{12}, is >− 40 dB, demonstrating a strong MC reduction between the radiating elements.

When the distance between the patches varies from d = 7 mm to d = 11 mm, S_{11} and S_{12} are greater than − 20 dB, and the optimized distance is d = 11 mm, which reduces the MC at the resonating frequencies.
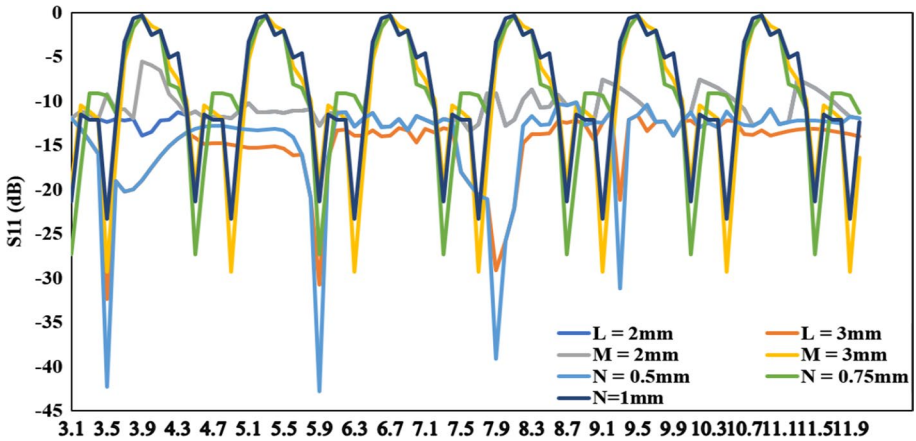
Fig. 10 S_{11} for different slit lengths and widths of the MIMO design

2.3.2 Effect on Varying Slit Lengths L, M, and N

Slit lengths L, M, and width N variations on the patch will significantly change the antenna analysis parameters like S_{11}, S_{12}, gain, and directivity. Figure 10 shows that S_{11} increases by 15 dB, with L, M, and width N variation.

3 Results and Discussion

This section presents the simulated and measured results for the design proposed. The proposed design analyses the envelope correlation co-efficient, diversity gain, and radiation efficiency.
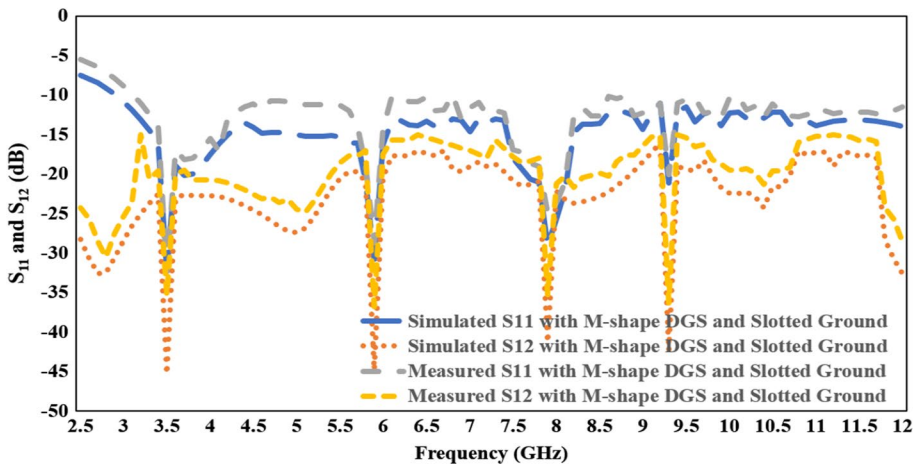

Fig. 11 S_{11} and S_{12} of the proposed MIMO design (Simulated and Measured)

3.1 Scattering Parameters and Radiation Analysis of The Design

The design is validated by fabricating the antenna, and the results measured are attained with Keysight (9916A) VNA. Figure 11 shows the measured and simulated S-parameters. The proposed design IBW is 7.6 GHz, with S_{12} below -35 dB.

Figure 12 shows the measurement setup for measurements of the proposed design. The measurements are taken by considering the Horn antenna as a transmitter and the proposed structure as a receiver. The distance between the two antennas is maintained at 2D2/λ, where D is the substrate width, and λ is the wavelength of the smallest resonating frequency of the UWB range. After simulating the equivalent circuit, R = 1 KΩ, L = 5.5 nH, and C = 10 pF. The figure reveals that the UWB band is a parallel combination of R, L, and C for the entire 2.5–12 GHz. The two parallel LC circuits in parallel represent the M-shape DGS structure.

Radiation plots at the resonant frequency are depicted in Fig. 13. A gain of 4.55 dBi is achieved for the prototype fabricated, and the simulated gain is 5.50 dBi, as shown in Figs. 14, 15 demonstrates the co-polarization and cross-polarization plots in E-plane and H-plane which indicates the desired orthogonal polarization of the proposed design radiation pattern. Figure 16 shows the fabricated model of the proposed design. The equivalent circuit is proposed in Fig. 17. A comparison of different techniques with the proposed design is shown in Table 2. Table 2 indicates the comparison of the proposed design with the existing works. As seen from Table 2, the proposed design resonates at four different frequencies over the UWB range compared to other related works. As seen from the Table 2, the proposed design provides multiple applications as the proposed design resonates at four different resonating frequencies.

3.2 MIMO Parameters for the Proposed Structure

The validation of the design is done by analyzing Envelope Correlation Co-efficient (ECC) and Diversity Gain (DG). The simulation and measured parameters are compared. ECC analysis is performed using S-parameters as mentioned [29]; ECC is < 0.05 and is shown in Fig. 18. DG with 9.9 dB is shown in Fig. 19. The ECC based on S_{12} is given in Eq. (1) in terms of field-based equation and specifies the radiation patterns of two radiating elements correlation.
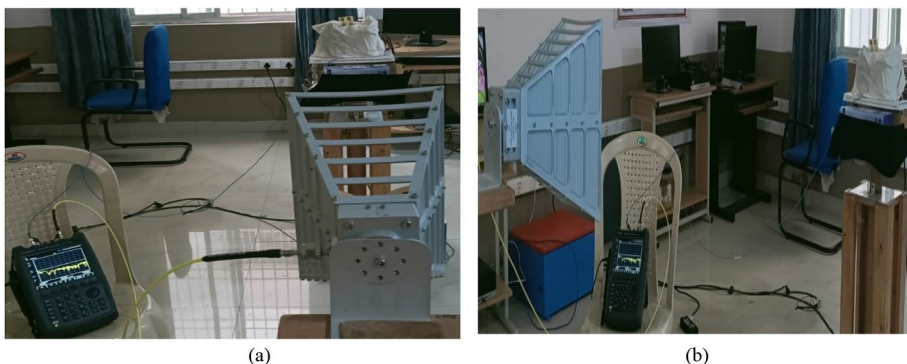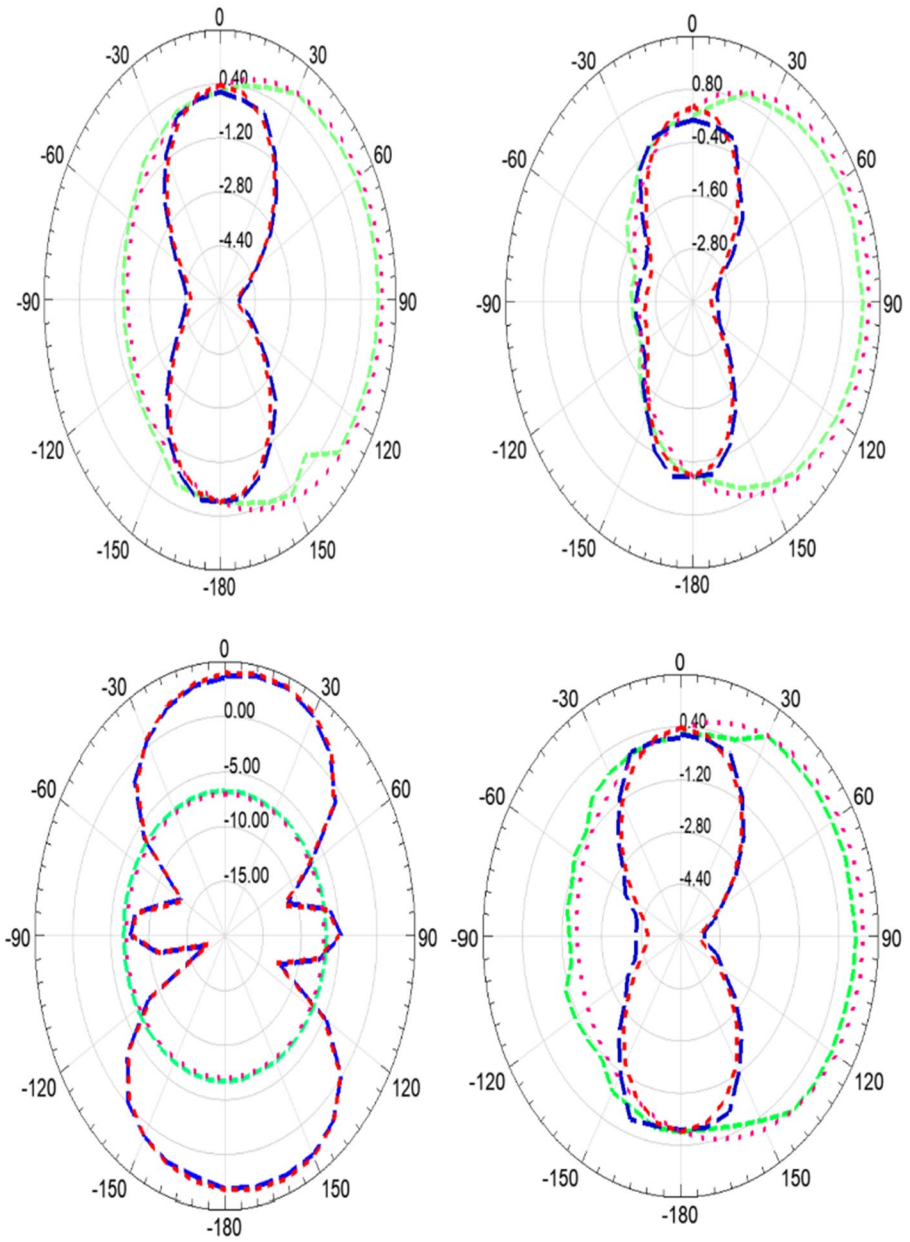

(a)   (b)

Fig. 12 Measurement setup for the measurements of the proposed design

Fig. 13 2-Dimensional radiation plots at the design's resonating frequencies in E-and H-Planes (red color & blue color: simulated and measured in E-Plane, pink color, and green color: simulated and measured in H-Plane)
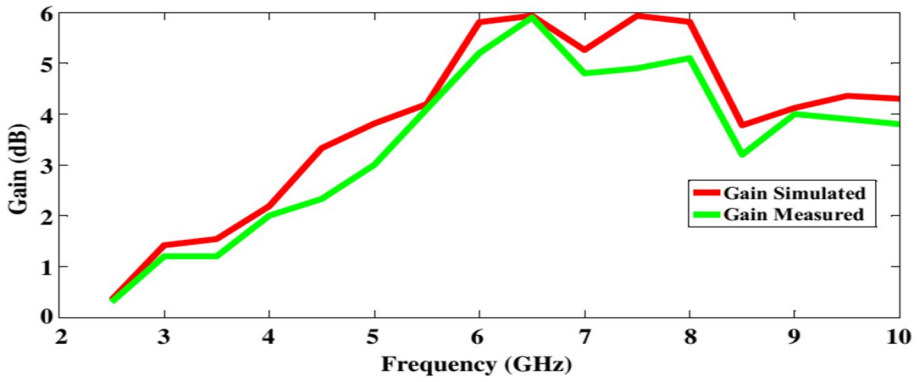
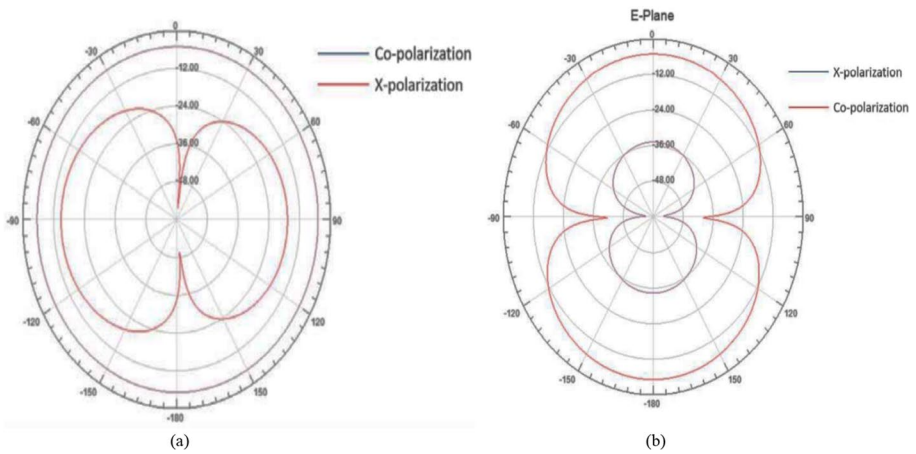**Fig. 14** Simulated and measured gain of the proposed MIMO design

Fig. 15 **a** Co- and cross-polarization at 3.45 GHz in H-Plane **b** Co and cross-polarization at 3.45 GHz in E-Plane
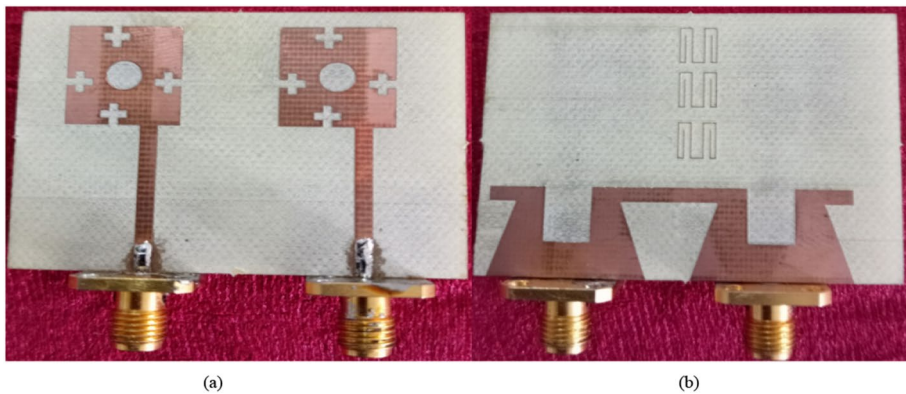

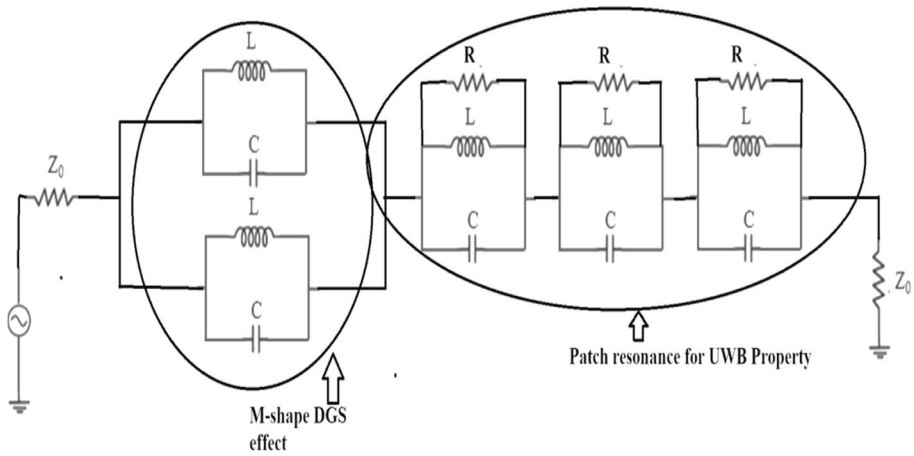**Fig. 16** Fabricated Design, **a** front view, **b** back view

Fig. 17 Equivalent circuit of the proposed design

$$\rho_e = \frac{\left|\int_0^{2\pi}\int_0^{2\pi}\left(XPR \cdot E_{\theta 1} \cdot E_{\theta 2}^* \cdot P_\theta + E_{\varphi 1} \cdot E_{\varphi 2}^* \cdot P_\varphi\right)d\Omega\right|^2}{\int_0^{2\pi}\int_0^{\pi}\left(XPR \cdot E_{\theta 1}E_{\theta 2}^* \cdot P_\theta + E_{\phi 2} \cdot E_{\varphi 2}^* \cdot P_\varphi\right) \times \int_0^{2\pi}\int_0^{2\pi}\left(XPR \cdot E_{\theta 1} \cdot E_{\theta 2}^* \cdot P_\theta + E_{\varphi 1} \cdot E_{\varphi 2}^* \cdot P_\varphi\right)d\Omega}$$

(1)

The formula gives DG based on the ECC.

$$DG = 10\sqrt{1 - ECC} \tag{2}$$

Irrespective of the antennas used, DG depends on BER, and the radiation efficiency is shown in Fig. 20 and reveals that the RE > 95%. The efficiency is calculated using a formula.

$$Effciency = \left(1 - |TACR|^2\right) * Radiation\ effciency \tag{3}$$

Table 2 Comparative analysis of the proposed work with related research works

| Reference	Antenna Dimensions (mm)	S_{11} (dB)	S_{12} (dB)	Frequency (GHz)	Substrate used
[2]	28×58×1.6	>−10	>−20	UWB (2.1–12.9)	FR-4
[3]	60×40×1.6	−48 & −19	−54 & −40	2.4 & 5.2	FR-4
[4]	34×80×1.6	>−15	>−15	3.1–10.9	FR-4
[9]	22×34×1.6	−18.29	−55.12	8.97	FR-4
[10]	15×20×1.6	>−10	-	(2.34–2.46), 4.61–5.92 and 9–9.9	FR-4
[11]	30×30×3.81	−35	−56	2.57	Rogers TMM 6
[12]	28×55×1.6	>−10	−29	(2.35–2.5) and (3.2–3.85)	FR-4
[14]	30×50×1.6	>−10	>−20	UWB	FR-4
[16]	30×30×3.81	−35	−35	2.2	Rogers TMM 6
[17]	30×36×3.8	>−10	−42	5.8	Rogers RT/duroid 5880
Proposed method	36×50×1.6	>−10 at 3.5, 5.9, 7.9 and 9.3 GHz	>−15 at 3.5, 5.9, 7.9 and 9.3 GHz	UWB (2.5–12)	FR-4
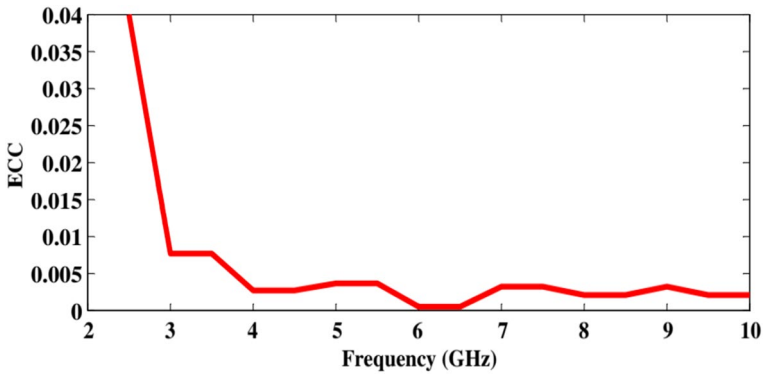
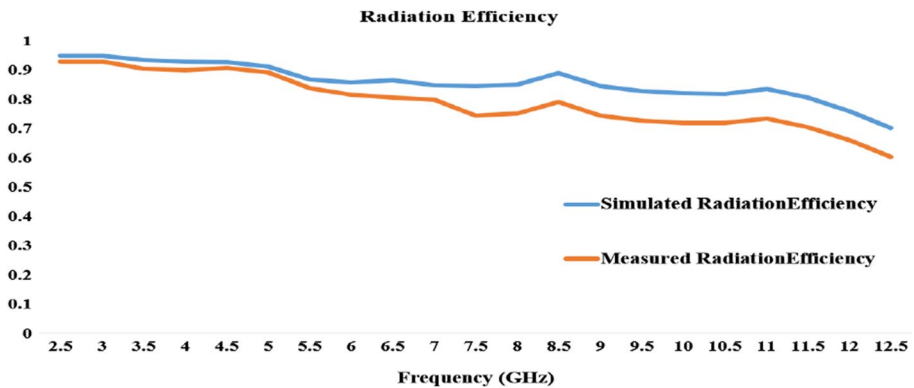**Fig. 18** Simulated ECC
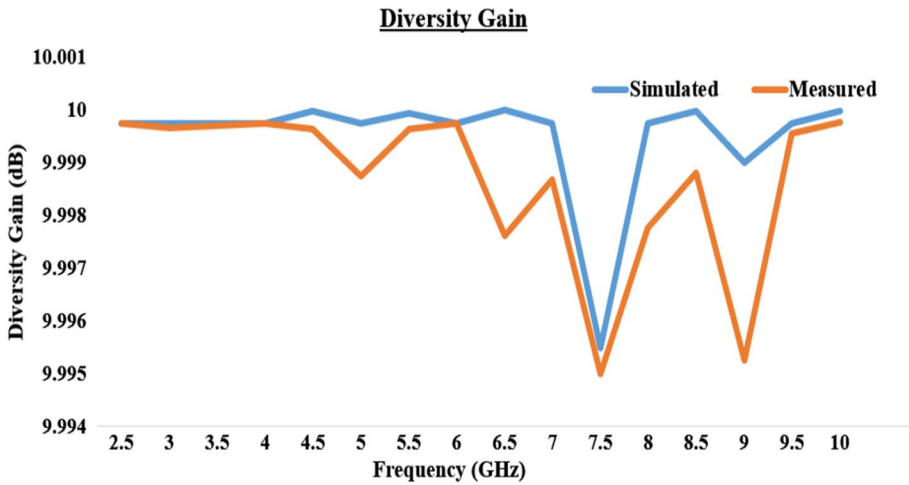
Fig. 19 Simulated and measured DG

Fig. 20 Radiation efficiency (RE) (%) of the proposed design

4 Conclusion

A slotted MIMO with M-shape DGS and slotted ground with 36×50 mm^2 is analyzed. Two slotted MIMO antenna elements operate for the UWB band. To validate the design, fabrication of a two-element structure is done and tested. The edge-to-edge gap is 0.215λo. An M-shaped DGS and slotted ground improve isolation at 3.45, 5.89, 7.95, and 9.30 GHz with $S_{12} > -15$ dB. Isolation enhancement is improved by etching an M-shape DGS on the slotted ground, and the gain is 4.95 dBi, DG > 9.9 dB, and ECC < 0.05, for the entire UWB.

Data availability Enquiries about data availability should be directed to the authors.

Declarations

Conflit of interest We hereby declare that we are the sole authors of this article. To the best of my knowledge, this article contains no material previously published by any other person except where due acknowledgement has been made.

References

1. Tiwari, R. N., Singh, P., Kanaujia, B. K., & Pandit, A. K. (2020). A coalesced kite shaped monopole antenna for UWB technology. *Wireless Personal Communications, 114*(4), 3031–3048.
2. Addepalli, T., & Anitha, V. R. (2019). Design and parametric analysis of hexagonal shaped MIMO patch antenna for S-band, WLAN, UWB, and X-band applications. *Progress in Electromagnetics Research C, 97*, 227–240.
3. Vasu Babu, K., & Anuradha, B. (2020). Design of multi-band minkowski MIMO antenna to reduce the mutual coupling. *Journal of King Saud University Engineering Sciences, 32*, 51–57.
4. Sahoo, A. B., Mishra, G. P., & Mangaraj, B. B. (2021). Design and performance study of single and multi-layered fractal based miniaturized patch antennas for 2.4 GHz applications journal of microwaves. *Opto-electronics and Electromagnetic Applications, 20*, 274–296.
5. Mishra, G. P., & Mangaraj, B. B. (2020). Highly compact microstrip patch design based on improved capacitive minkowski fractal defected ground structure. *International Journal of Electronics and Communication, AEU, 115*, 153049.
6. Naktong, W., & Ruengwaree, A. (2020). Four-port rectangular monopole antenna for UWB-MIMO applications. *Progress in Electromagnetics Research B, 87*, 19–38.
7. Jena, M. R., Sahoo, S., Mishra, G. P., & Mangaraj, B. B. (2021). Miniaturised band notched printed LPDA design with meander fractal dipole for UWB communication. *International Journal of Electronics, 108*(1), 21–44.
8. S. Sahoo, G P Mishra, Manas Ranjan Jena, and Biswa Binayak Mangaraj, 2019 Sub-sectional Tapered Printed-LPDA Design with WLAN, WiMAX Notch Bands for UWB Communication Systems, International Conference on Intelligent Computing and Communication Technologies, ICICCT, pp: 717-727
9. Mondal, K., & Sarkar, P. P. (2019). gain and bandwidth enhancement of microstrip patch antenna for WiMAX and WLAN applications. *IETE Journal of Research, 67*, 726–734.
10. Park, J. D., Rahman, M., & Chen, H. N. (2019). Isolation Enhancement of Wide-Band MIMO Array Antennas utilizing resistive loading. *IEEE Access, 7*, 81020–81026.
11. Rajiv, P., Mishra, G. P., Mangaraj, B. B., & Narayan, A. (2020). An improved compact antenna design proposed for 5G cellular band international journal of sensors. *Wireless Communications and Control, 10*, 886–899.
12. Kumar, N., & Kommuri, U. K. (2018). MIMO antenna mutual coupling reduction for WLAN using spiro meander line UC-EBG. *Progress in Electromagnetics Research C, 80*, 65–77.
13. Sahoo, A. B., & Mangaraj, B. B. (2020). A miniaturized electromagnetically coupled patch antenna design using an eroded ground plane. *Microwave and Optical Technology Letters, 62*, 3589–3600.

14. Shinde, J. P., & Shinde, P. N. (2016). M-shape electromagnetic-bandgap structures for enhancement in antenna performance. *International Journal of Electronics and Communications-(AEU), 70*, 842–849.

15. Sahoo, A. B., Mishra, G. P., & Mangaraj, B. B. (2019). Optimal design of compact dual-band slot antenna using particle swarm optimization for WLAN and WiMAX applications. *Recent Advances in Electrical and Electronic Engineering, 12*, 425–431.

16. Hao, C., Zheng, H., Zhang, J., & Sun, X. (2020). The deployment of stub structures for mutual coupling reduction in MIMO antenna applications. *Progress in Electromagnetics Research Letters, 92*, 39–45.

17. Mishra, G. P., Sahoo, A. B., Hota, S., & Mangaraj, B. B. (2019). Direct and electromagnetically coupled compact microstrip antenna design with modified fractal DGS. *International Journal of RF and Microwave Computer-Aided Engineering, 29*, 1–18.

18. Mishra, G. P., & Mangaraj, B. B. (2019). Miniaturized microstrip patch design based on highly capacitive defected ground structure with a fractal boundary for X-band microwave communications. *IET Microwaves, Antennas and Propagation, 13*, 1593–1601.

19. Asnani, V., & Baudha, S. (2019). Triple band microstrip patch antenna useful for Wi-Fi and WiMAX. *IETE Journal of Research, 68*, 34–41.

20. Wei, K., Li, J., Wang, L., Xing, Z., & Rui, Xu. (2016). S-shaped periodic defected ground structures to reduce microstrip antenna array mutual coupling. *Electronics Letters, 52*, 1288–1290.

21. Biswas, A. K., & Chakraborty, U. (2018). Reduced mutual coupling of compact MIMO antenna designed for WLAN and WiMAX applications. *International Journal of RF and Microwave Computer-Aided Engineering, 29*, 1–10.

22. Xiao, S., Tang, M.-C., Bai, Y.-Y., Gao, S., & Wang, B.-Z. (2011). Mutual coupling suppression in microstrip array using defected ground structure. *IET Microwaves, Antennas & Propagation, 5*, 1488–1494.

23. Iqbal, A., Saraereh, O. A., Ahmad, A. W., & Bashir, S. (2017). Mutual coupling reduction using F-shaped stubs in UWB-MIMO antenna. *IEEE Access, 6*, 2755–2759.

24. Hota, S., Baudha, S., Mangaraj, B. B., & Varun Yadav, M. (2020). A novel compact planar antenna for ultra-wideband application. *Journal of Electromagnetic Waves and Applications, 34*(1), 116–128.

25. Ghosh, J., Mitra, D., & Das, S. (2019). Mutual coupling reduction of slot antenna array by controlling surface wave propagation. *IEEE Transactions on Antennas and Propagation, 67*, 1352–1357.

26. Wei, K., Li, J.-Y., Wang, L., Xing, Z.-J., & Rui, Xu. (2016). Mutual coupling reduction by novel fractal defected ground structure bandgap filter. *IEEE Transactions on Antennas and Propagation, 64*, 4328–4335.

27. Sun, X. B., & Cao, M. Y. (2017). Low mutual coupling antenna array for WLAN application. *Electronics letters, 53*(6), 368–370.

28. Abdullah, Md., Li, Q., Wei Xue, G., Peng, Y. H., & Chen, X. (2019). Isolation enhancement of MIMO antennas using shorting pins. *Journal of Electromagnetic Waves and Applications, 33*, 1249–1263.

29. Biswas, A. K., Kundu, A., Bhattacharjee, A. K., & Chakraborty, U. (2019). Isolator-Based Mutual Coupling Reduction of H-shaped Patches in MIMO Antenna Applications. *Advances in Computer, Communication, and Control* (1st ed., Vol. 41, pp. 361–366). Springer, Singapore: Lecture Notes in Networks and Systems.

30. Luo, C.-M., Hong, J.-S., Member, I. E. E. E., & Zhong, L.-L. (2015). Isolation enhancement of a very compact UWB-MIMO slot antenna with two defected ground structures. *IEEE Antennas and Wireless Propagation Letters, 14*, 1766–1769.

31. Mohanty, A., & Sahu, S. (2019). High isolation two-port compact MIMO fractal antenna with Wi-Max and X-band suppression characteristics. *International Journal of RF and Microwave Computer-Aided Engineering, 30*, e22021.

32. Anitha, R., Sarin, V. P., Mohanan, P., & Vasudevan, K. (2014). Enhanced isolation with defected ground structure in MIMO antenna. *Electronic Letters, 50*, 1784–1786.

33. Yang, Z., Xiao, J., & Ye, Q. (2020). Enhancing MIMO antenna isolation characteristic by manipulating the propagation of surface waves. *IEEE Access, 8*, 115572–115581.

34. Prasad, K. V., & Prasad, M. V. (2021). Mutual Coupling Reduction between Slotted-T MIMO Elements for UWB Applications. *Progress In Electromagnetics Research C, 107*, 203–217.

35. Padarti, V. K., & Rao, N. V. (2020). adaptive SOICAF algorithm for PAPR mitigation in OFDM systems. *Wireless Personal Communication, 113*, 927–943. https://doi.org/10.1007/s11277-020-07260-y

36. Kudumu, P. V., & Mokkapati, V. S. P. (2020). A Slot-shaped EBG structure for improving the Isolation between Patch Arrays. *Internal Journal Microw Optical Techology, 15*, 269–278.

K. Vara Prasad received his Ph.D., from Acharya Nagarjuna University, College of Engineering, Guntur, M.Tech, from Srinidhi Institute of Science and Technology, Hyderabad. He is currently working as an assistant professor in VR Siddhartha Engineering College, Vijayawada, India. His research interests include MIMO, EBG, CSRR, and mutual coupling reduction in MIMO antennas. He is a member of IETE. He has published 15 papers in national and international journals in the area of Ultra-wideband Antennas.

Venkata Siva Prasad Makkapati completed his Doctoral degree and M. Tech in 2012 and 1989. Presently he is working as a Professor in R V R & JC College of Engineering and Technology. He had published papers in various National and International journals. He is a fellow of IETE